

Random Vibration Analysis of Stiffened Honeycomb Panels with Beveled Edges

J. Soovere*

Lockheed-California Company, Burbank, California

A semi-empirical theory is presented for predicting the dynamic strains in the face sheets of honeycomb panels subjected to random acoustic loading. The honeycomb panels are constructed with beveled edges that terminate in a solid panel edge strip around the panel periphery for ease of attachment to the substructure with countersunk fasteners. It is shown that the rotation of the beveled edges introduces a linear dynamic membrane strain into the inner face sheet superimposed on the bending strain. Furthermore, the extensional stiffness of the beveled edge closeout pan is shown to provide the dominant contribution to the honeycomb core shear stiffness exceeding that of the core alone by almost an order of magnitude. Good agreement is obtained between the predicted and measured strains, the latter taken from existing test data representing a wide range of honeycomb panel dimensions.

Nomenclature

| | |
|----------------------------|---|
| \bar{a}, \bar{b} | = panel overall length and width, respectively |
| a, b | = equivalent panel length and width, respectively |
| \bar{B}_y, \bar{B}_{y_0} | = inner and outer face sheet strain parameters defined by Eqs. (44) and (45), respectively |
| b, b_i | = equivalent honeycomb beam length and inner face sheet length, respectively |
| c | = speed of sound in air |
| E, E_p | = Young's modulus of both face sheets and of the closeout pan, respectively |
| f_r | = natural frequency of the m, nth mode |
| G, G' | = actual and equivalent shear modulus, respectively, of the honeycomb core |
| G_f | = constant power spectral density of the random acoustic excitation |
| h | = honeycomb core height |
| j_{rr} | = direct joint acceptance for the m, nth mode |
| K' | = shear-related parameter, Eq. (33) |
| ℓ | = small part of the solid panel edge width (Fig. 6) |
| ℓ_p | = length of the closeout pan |
| M | = mass per unit area of honeycomb panel, Eq. (3) |
| M_{AB} | = bending moment at beveled edge |
| m, n | = mode number parallel to the x and y axes, respectively |
| q, q' | = shear stress and equivalent shear stress, respectively |
| r | = subscript denoting the m, nth mode |
| s | = solid panel edge width |
| T_A, T'_B | = unreacted forces per unit length at beveled edge of honeycomb beam (Fig. 7) |
| T_i, T_o | = in-plane forces per unit length in the inner and outer face sheets, respectively, at the beveled edge of honeycomb beam |
| T_e, T_p | = in-plane forces per unit length in the solid panel edge and pan, respectively, of honeycomb beam |
| $T(y)$ | = variable in-plane force in the inner face sheet of honeycomb beam parallel to the y axis |
| t, t_{ad}, t_p | = thickness of each face sheet, each adhesive layer, and the pan, respectively |

| | |
|--------------------------------|--|
| u, v, w | = displacement parallel to the x, y , and z axes, respectively (Fig. 3) |
| $v(y)$ | = variable in-plane displacement of inner face sheet of honeycomb beam parallel to the y axis |
| w_n | = modal intensity for n th mode of honeycomb beam |
| $w_r(x, y)$ | = mode shape of honeycomb panel m, nth mode |
| x, y, z | = coordinate axes (Fig. 3) |
| γ_B | = shear angle of the honeycomb core at the beveled edge |
| $\gamma(y)$ | = variable shear angle of the honeycomb core |
| δ_r | = viscous damping ratio of m, nth mode |
| δ_o, δ_B | = lateral displacement of panel edge and corner of beveled edge, respectively (Fig. 7) |
| $\bar{\epsilon}(x, y)$ | = general expression for the root-mean-square (rms) strain |
| $\epsilon(y)$ | = variable in-plane strain in the inner face sheet of honeycomb beam parallel to y axis |
| $\epsilon_{Bo}, \epsilon_{Bi}$ | = inner and outer face sheet strain, respectively, in honeycomb beam due to bending |
| $\epsilon_{Mi}, \epsilon_{Mo}$ | = membrane strain in inner and outer face sheets of honeycomb beam with extensionally rigid pans |
| ϵ_{Mc} | = membrane strain at the center of the inner face sheet with extensionally flexible pans |
| ϵ_p | = in-plane strain in the pan of honeycomb beam |
| $\epsilon_r(x, y)$ | = modal strain in honeycomb panel |
| ϵ_{ry} | = modal surface strain at panel center parallel to the y axis |
| ϵ_{yci} | = inner face sheet rms strain, including membrane strain, at center of panel parallel to the y axis |
| ν | = face sheet Poisson's ratio |
| $\rho_{ad}, \rho_R, \rho_f$ | = density of the adhesive, the honeycomb core, and the face sheets, respectively |
| χ | = beveled edge angle |
| ψ_A, ψ_o | = rotation of the honeycomb beam at the beveled edge and at the end of a short length of the solid panel edge, respectively (Fig. 7) |

Introduction

HONEYCOMB panels are often used in lightly loaded areas on aircraft, such as fairings, wing trailing-edge structures, and control surfaces. These honeycomb panels are usually constructed with beveled edges that terminate in a solid panel edge strip around the periphery of the panel (Fig. 1) for ease of attachment to the substructure with fasteners. Some of these panels are located in areas of the aircraft subjected to a high-level jet noise environment. This broadband

Submitted April 11, 1985; presented as Paper 85-0603 at the AIAA 26th Structures, Structural Dynamics and Materials Conference, Orlando, FL, April 15-17, 1985; revision received Jan. 17, 1986. Copyright © 1985 by Lockheed Corporation. Published by the American Institute of Aeronautics and Astronautics, Inc., with permission.

*Senior Research Specialist.

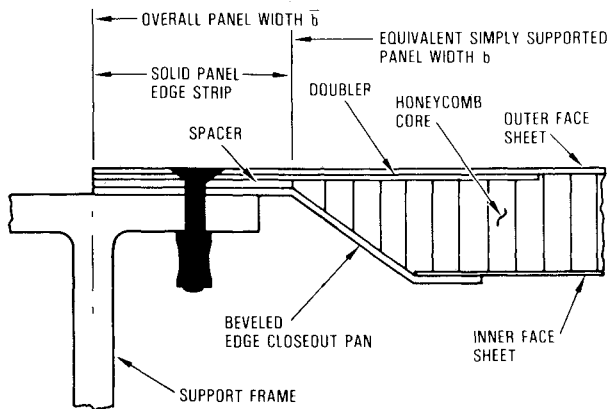
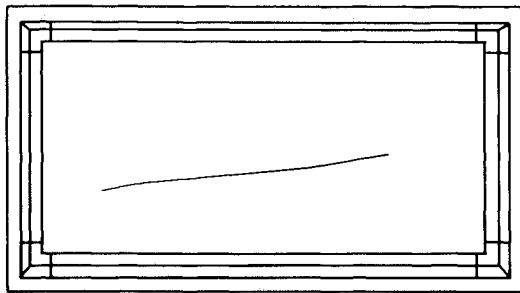


Fig. 1 Typical honeycomb panel edge design.

Fig. 2 Typical inner face sheet fatigue crack in honeycomb panel.²

random jet noise has produced high cycle fatigue failures in these panels¹ along the fastener lines and in the face sheets, usually the inner face sheet (Fig. 2), by exciting the panels at their dominant resonant modes. The dominant response is usually obtained in the fundamental panel mode.

The current semiempirical method² for predicting the root-mean-square (rms) stresses (and strains) in honeycomb panels subjected to random acoustic loading is based on clamped edges, a fundamental single-mode response, and a fully correlated acoustic field over the panel surface. In this method, the theoretically correct exponents of well-established structural, excitation, and damping parameters were allowed to vary in the least-squares curve fit to the test data. The resulting exponents differed significantly from their theoretically correct values, even when the measured response was due to a single mode. Consequently, the above analytical model must either be incorrect or incomplete. For example, the theory does not explain the reason for the higher face sheet strains being measured on the inner face sheet of honeycomb panels with beveled edges.³

This paper presents a semiempirical theory for predicting the rms strains in the face sheets of stiffened honeycomb panels when subjected to random acoustic loading. The theory includes the effect of beveled edges on the honeycomb panel strain distribution. The analysis is restricted to honeycomb panels, with isotropic face sheets, exhibiting a predominant fundamental mode response. An extension of this theory, for predicting the rms strains in the honeycomb panel edges, is described in Ref. 4.

Honeycomb Panel Natural Frequencies

It was shown by Sweers³ that the natural frequencies of rigidly mounted honeycomb panel modes could be predicted with reasonable accuracy using equivalent simply supported honeycomb panel theory in which the honeycomb core is assumed to be infinitely stiff in shear. These honeycomb panels are also assumed to be simply supported at the base of the beveled edges (Fig. 1). The length a and width b of such an equivalent simply supported honeycomb panel are

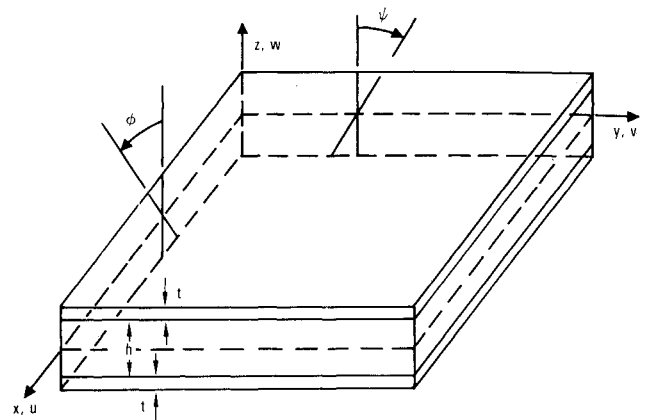


Fig. 3 Honeycomb panel coordinate axes.

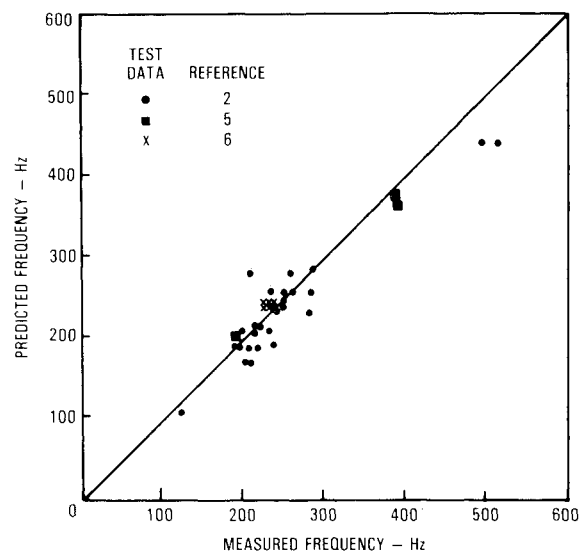


Fig. 4 Comparison of predicted and measured fundamental mode natural frequency of stiffened aluminum honeycomb panels.

related to the overall length \bar{a} and width \bar{b} by

$$a = \bar{a} - 2s, \quad b = \bar{b} - 2s \quad (1)$$

where s is the width of the solid panel edges. The expression for the m, n th mode natural frequency of the equivalent simply supported honeycomb panel, with isotropic face sheets and honeycomb core that is infinitely stiff in shear, is given in Hz by

$$f_r = \frac{\pi}{2} \{h + t\} \left\{ \left(\frac{m}{a} \right)^2 + \left(\frac{n}{b} \right)^2 \right\} \left\{ \frac{Et}{2(1-\nu^2)M} \right\}^{1/2} \quad (2)$$

where M , the mass per unit area, is

$$M = 2\rho_f t + \rho_c h + 2\rho_{ad} t_{ad} \quad (3)$$

and h and ρ_c are the height and density, respectively, of the honeycomb core; t , ρ_f , E , and ν the face sheet thickness, density, Young's modulus, and Poisson's ratio, respectively; t_{ad} and ρ_{ad} the adhesive film thickness and density, respectively; and m and n the mode numbers in the panel length and width directions, respectively. The coordinate axes are illustrated in Fig. 3.

The fundamental mode natural frequencies predicted by Eq. (2) appear to be in good agreement with the measured frequencies for the wide range of honeycomb panels in Refs. 2, 5, and 6, as illustrated in Fig. 4. The use of the empiri-

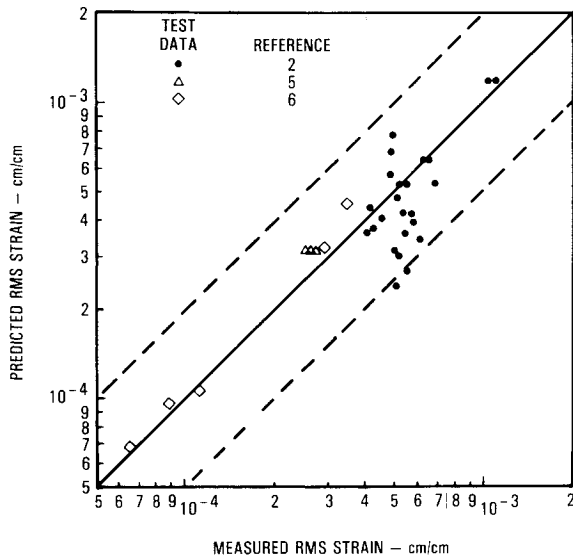


Fig. 5 Comparison of predicted and measured aluminum honeycomb panel center rms strain due to random acoustic loading.

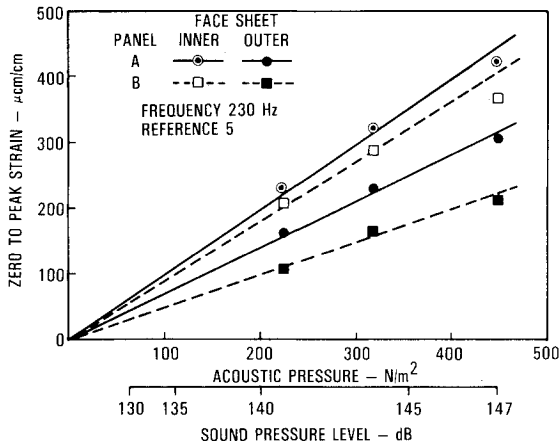


Fig. 6 Typical variation of inner and outer face sheet strains at resonance with discrete frequency acoustic pressure.

cally derived equivalent simply supported mode shapes has both simplified the theory and enabled existing expressions⁷ for the generalized force of acoustically excited simply supported panels to be used in the subsequent analysis. The concept of equivalent simply supported panels is not new, having previously been used by a number of authors.⁸⁻¹⁰

Face Sheet Strain Due to Random Acoustic Loading

The theory for predicting the response of a simply supported panel to random acoustic loading is well established.^{7,11,12} Consequently, only the final forms of the equations are included in this paper. In many acoustic fatigue test reports, the rms strains are listed only at the failure locations. In the honeycomb panels, tested in Ref. 2, the face sheet failures occurred primarily in the inner face sheets parallel to the longest panel sides (see Fig. 2). The critical rms strain was measured at the panel center, parallel to the y axis (Fig. 2). Consequently, expressions for the rms strain are developed in this paper primarily for this location.

The general expression for the rms strain $\bar{\epsilon}(x,y)$ of a panel exhibiting a single mode response to a random excitation with a constant power spectral density G_f is

$$\bar{\epsilon}(x,y) = \left\{ \frac{G_f}{2\pi^4 M^2} \frac{\epsilon_r^2(x,y) j_{rr}^2}{\delta_r f_r^3} \right\}^{1/2} \quad (4)$$

where $\epsilon_r(x,y)$ is the modal strain, j_{rr} the direct joint acceptance, δ_r the viscous damping ratio, and ω_r the natural circular frequency. For a simply supported panel excited by an acoustic progressive wave moving parallel to the x axis,

$$j_{rr}^2 = \frac{8}{\pi^4 m^2 n^2} \frac{\{1 - \cos(m\pi) \cos(\omega_r a/c)\}}{\{1 - (\omega_r a/m\pi c)^2\}^2} \quad n \text{ odd}$$

$$= 0 \quad n \text{ even} \quad (5)$$

where c is the speed of sound in air. The modal strain $\epsilon_r(x,y)$ in Eq. (4) is replaced by $\epsilon_{ry}(a/2, b/2)$ when measured at the center of the panel, parallel to the y axis. At the surface of the honeycomb panel, where $z = \pm(h+2t)/2$, this strain becomes simply

$$\epsilon_{ry}(a/2, b/2) = \pm \left(\frac{h+2t}{2} \right) \frac{\partial^2 w_r(x,y)}{\partial y^2} \bigg|_{\substack{x=a/2 \\ y=b/2}}$$

$$= \pm \left(\frac{h+2t}{2} \right) \left(\frac{n\pi}{b} \right)^2 \quad (6)$$

The plus and minus signs in Eq. (6) refer to the inner and the outer face sheets, respectively, and $w_r(x,y)$ is the equivalent simply supported mode shape given by

$$w_r(x,y) = \sin \frac{m\pi x}{a} \sin \frac{n\pi y}{b} \quad (7)$$

The rigidly mounted honeycomb panels described in Refs. 2, 5, and 6 were tested in an acoustic progressive wave test facility using band-limited constant spectrum level random noise. The bandwidth of the random noise was selected so as to excite only the fundamental mode ($m=n=1$) of each panel. The expression for the rms strain at the panel center, when subjected to the above excitation, becomes

$$\bar{\epsilon}_{yc} = \pm \frac{1}{\pi^2} \frac{(h+2t)}{b^2 M} \left(\frac{G_f}{\delta_r} \right)^{1/2} \frac{1}{f_r^{3/2}} \frac{\{1 + \cos(2\pi f_r a/c)\}^{1/2}}{\{1 - (2f_r a/c)^2\}} \quad (8)$$

The agreement between the measured inner face sheet strains at the failure locations and those predicted by Eq. (8) appears to be quite good, as shown in Fig. 5. There is, however, a discrepancy between the inner and outer face sheet strains, as illustrated in Fig. 6. Equation (8) overestimates the strain in the outer face sheet by almost a factor of 2. Consequently, it must be concluded that the simple theory, as represented by Eq. (8), is incorrect as it stands.

Effect of Beveled Edge on Face Sheet Strain Ratio

It is shown in this section that the rotation of the beveled edges is responsible for introducing a linear dynamic membrane strain into the inner face sheet of rigidly mounted honeycomb panels superimposed on the dynamic bending strain. For simplicity, the basic theory for predicting the inner face sheet membrane strain is developed for a honeycomb beam with beveled edges using the equivalent simply supported mode shapes. A beveled edge of the honeycomb beam is illustrated schematically in Fig. 7, just before and at an instant of time after deflection, during bending vibration. Lateral frame flexibility, represented by the displacement δ_o , and a small section OA of length ℓ of the solid panel edge are included for generality. The closeout pan AB and the solid panel edge are assumed to be extensionally rigid. With an extensionally rigid pan, no core shear is possible. Rotation of the test frame is also excluded from the analysis since it does not affect the basic results.

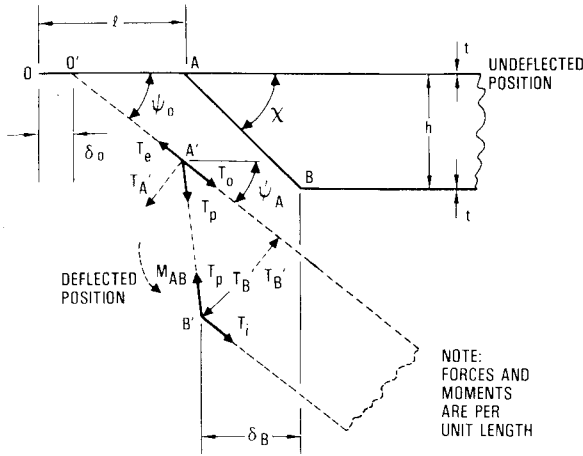


Fig. 7 Displacements, forces, and moments at the honeycomb panel beveled edge.

A small rotation ψ_o at one beveled edge and $-\psi_o$ at the other beveled edge during symmetric bending of the honeycomb beam changes the length of the outer face sheet by $2\delta_A$. This change in length, represented by the horizontal displacement of point A to A' in Fig. 7, at each end of the beam, is given by

$$2\delta_A = 2(\ell - \ell \cos \psi_o - \delta_o) = -2\delta_o \quad (9)$$

Consequently, without any lateral frame flexibility, a small rotation of the beveled edges does not produce any extension in the outer face sheet. The only strain in the outer face sheet is, in this instance, due to the linear bending of the honeycomb beam, assuming small-deflection theory.

The corresponding change in the length of the inner face sheet $2\delta_B$, due to a small rotation of the beveled edges, is represented by the horizontal displacement of point B to B' at each end of the honeycomb beam and is given by

$$2\delta_B = 2\left\{\ell - \ell \cos \psi_o + \frac{h \cos \chi}{\sin \chi} - \frac{h \cos (\chi + \psi_A)}{\sin \chi} - \delta_o\right\} = 2h\psi_A - 2\delta_o \quad (10)$$

where χ is the beveled edge angle, h the height of the honeycomb core, and ψ_A the small rotation of the honeycomb beam at point A due to beam bending. Therefore, without frame lateral flexibility, the rotation of the beveled edge produces a linear extension in the inner face sheet, even for a very small rotation of the beveled edge.

The inner and outer face sheet strains, due to the rotation of the beveled edges, are obtained simply by dividing the extensions in Eqs. (9) and (10) by the corresponding face sheet lengths. The inner and outer face sheet strains are therefore given by

$$\epsilon_{Mi} = \frac{2h\psi_A - 2\delta_o}{b_i} \quad (11)$$

and

$$\epsilon_{Mo} = -\frac{2\delta_o}{b - 2\ell} \quad (12)$$

respectively, where b is the equivalent beam length and b_i is the length of the inner face sheet given by

$$b_i = b - 2\ell - 2h/\tan \chi \quad (13)$$

The strains in Eqs. (11) and (12) are linear dynamic membrane strains.

The dynamic bending strain at the center of the beam is required to derive the expression for the inner-to-outer-face-sheet strain ratio. The equivalent simply supported mode shape for the honeycomb beam is given by

$$w(y) = w_n \sin(n\pi y/b) \quad (14)$$

where w_n is the modal intensity for the n th bending mode and n is the mode number. With rigid beveled edge pans and therefore no core shear, $\psi = -\partial w/\partial y$. The surface bending strains at the center of the honeycomb beam are

$$\begin{aligned} \epsilon_{Bi} &= -\left(\frac{h}{2} + t\right) \left[\frac{\partial^2 w(y)}{\partial y^2} \right]_{y=b/2} \\ &= \left(\frac{h}{2} + t\right) \frac{n^2 \pi^2}{b^2} w_n \quad n = 1, 3, 5, \dots \end{aligned} \quad (15)$$

and

$$\epsilon_{Bo} = -\left(\frac{h}{2} + t\right) \frac{n^2 \pi^2}{b^2} w_n \quad n = 1, 3, 5, \dots \quad (16)$$

for the inner and outer face sheets, respectively. The corresponding rotation ψ_A at the beveled edge, as shown in Fig. 7, is

$$\psi_A = -\left[\frac{\partial w(y)}{\partial y} \right]_{y=\ell} = \frac{n\pi}{b} w_n \cos \frac{n\pi \ell}{b} \quad (17)$$

The expression for the rotation in Eq. (17) can now be substituted back into Eq. (11). The inner-to-outer-face-sheet dynamic strain ratio is obtained by dividing the sum of the inner face sheet membrane and bending strains by the sum of the outer face sheet membrane and bending strains. The positive value of the ratio is given by

$$\begin{aligned} \left| \frac{\epsilon_{Mi} + \epsilon_{Bi}}{\epsilon_{Mo} + \epsilon_{Bo}} \right| &= \left\{ 1 + \frac{4}{\pi n} \left[\frac{\cos \left(\frac{n\pi \ell}{b} \right) - \frac{b}{n\pi h} \left(\frac{\delta_o}{w_n} \right)}{\left(1 + \frac{2t}{h} \right) \left(1 - \frac{2\ell}{b} - \frac{2h}{b \tan \chi} \right)} \right] \right\} \\ &\div \left[1 + \frac{4b}{n^2 \pi^2 h \left(1 + \frac{2t}{h} \right) \left(1 - \frac{2\ell}{b} \right)} \left(\frac{\delta_o}{w_n} \right) \right] \end{aligned} \quad (18)$$

$$n = 1, 3, 5, \dots$$

Therefore, the membrane strain is shared between both face sheets with laterally flexible edge supports. For laterally rigid panel edge supports, this ratio reduces to

$$\left| \frac{\epsilon_{Mi} + \epsilon_{Bi}}{\epsilon_{Bo}} \right| = 1 + \frac{4}{n\pi} \left\{ \frac{\cos(n\pi \ell/b)}{\left(1 + \frac{2t}{h} \right) \left(1 - \frac{2\ell}{b} - \frac{2h}{b \tan \chi} \right)} \right\} \quad n = 1, 3, 5, \dots \quad (19)$$

Equation (19) can be further simplified by assuming that t is small compared to h and that both h and ℓ are small compared to b . Therefore,

$$\begin{aligned} \left| \frac{\epsilon_{Mi} + \epsilon_{Bi}}{\epsilon_{Bo}} \right| &= 1 + \frac{4}{n\pi} \quad n = 1, 3, 5, \dots \\ &= 2.273 \text{ for } n = 1, \text{ the fundamental mode} \end{aligned} \quad (20)$$

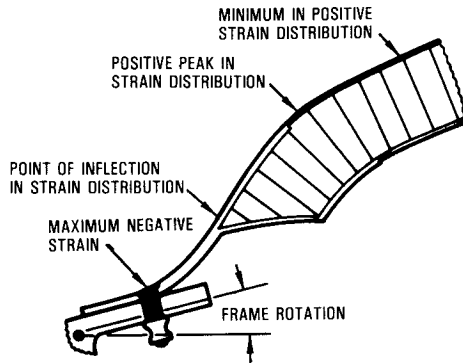


Fig. 8 Schematic illustration of honeycomb beam deformation at the beveled edge.

The above value is in good agreement with the ratio, between 2 and 2.5, quoted in Ref. 3 for the measured strain ratios.

Other Beveled Edge Effects

On examining the forces and moments in Fig. 7, it is seen that there is a resultant moment M_{AB} and an unreacted force T'_B at the beveled edges, both per unit length, that are given by

$$M_{AB} = T_i h \quad (21a)$$

and

$$T'_B = T_p \sin \chi = T_i \tan \chi \quad (21b)$$

where

$$T_i = \frac{2n\pi h t E \cos\left(\frac{n\pi \ell}{b}\right)}{b^2 \left(1 - \frac{2\ell}{b} - \frac{2h}{b \tan \chi}\right)} w_n \quad (22)$$

and E is the Young's modulus of both face sheets. A doubler (Fig. 1) is used in most honeycomb panels to resist the local distortion produced by this moment and force. The type of distortion obtained is illustrated schematically in Fig. 8, based on strain measurements made on a honeycomb beam in Ref. 2. A force per unit width T_e given by

$$T_e = \frac{Et \left[2h \frac{n\pi}{b} \cos\left(\frac{n\pi \ell}{b}\right) w_n - 2\delta_o \right]}{b \left(1 - \frac{2\ell}{b} - \frac{2h}{b \tan \chi}\right)} - \frac{Et 2\delta_o}{b \left(1 - \frac{2\ell}{b}\right)} \quad (23)$$

$$\approx Et \left\{ \frac{2n\pi h}{b^2} w_n - \frac{4\delta_o}{b} \right\}$$

is also present in the solid panel edges. Consequently, the strain produced by this force must be included in any theory⁴ for predicting the rms strain at the fastener line. Since the honeycomb panel and the edge support frames have both mass and stiffness in the lateral direction, the honeycomb panel bending vibration is coupled to the extensional vibration through Eq. (23). However, in most practical honeycomb panels, this coupling is small.

Extensional Flexibility of Closeout Pan

A shear angle can be introduced into the honeycomb core primarily through the extension and compression of the

panels, in the symmetric panel bending modes, excluding any local bending effects. The pans are therefore expected to provide considerable shear stiffness to the honeycomb core. The outer face sheet and the panel lateral edge supports are assumed to be rigid. These assumptions simplify the analysis and can be justified on the basis that no membrane strain is introduced into the outer face sheets with laterally rigid edge supports.

Each pan, under the membrane load, is extended in length from ℓ_p to $\ell_p + \delta \ell_p$. This extension produces a shear angle γ_B at one end of the inner face sheet in a direction opposite the rotation ψ in Fig. 8 and an angle $-\gamma_B$ in the same direction as ψ at the other end. The extension $2\delta_B$ of the inner face sheet [Eq. (10)], due to the rotation of the beveled edges, is now given by

$$2\delta_B = 2 \left\{ h\psi_A - h\epsilon_p \frac{\cos \chi}{\sin \chi} \right\} \quad (24)$$

where the strain ϵ_p in the pan is equal to $\delta \ell_p / \ell_p$. From geometric considerations, the strain and the shear angle are related by

$$\epsilon_p = \gamma_B \cos \chi \sin \chi \quad (25)$$

The equilibrium of the forces per unit length acting at B yields the equation

$$T_p \cos \chi = T_i - \int_0^{b/2} q dy \quad (26)$$

where q is the shear stress and

$$T_i = Et 2\delta_B / b_i, \quad T_p = E_p t_p \epsilon_p \quad (27)$$

In the above equations E_p and t_p are the Young's modulus and thickness, respectively, of the pan.

The membrane force per unit length $T(y)$, at a location y along the inner face sheet, is related to the shear stress q and shear angle $\gamma(y)$ in the honeycomb core by

$$\frac{\partial T(y)}{\partial y} = q = G\gamma(y) \quad (28)$$

In the above equations, G is the shear modulus of the core. Since

$$\frac{\partial \epsilon(y)}{\partial y} = \frac{1}{Et} \frac{\partial T(y)}{\partial y} = \frac{\partial^2 v}{\partial y^2} \quad (29)$$

and

$$v(y) = \gamma(y) h \quad (30)$$

then

$$\frac{\partial^2 v(y)}{\partial y^2} = \frac{G}{Eth} v(y) \quad (31)$$

The solution to Eq. (31) is given by

$$v(y) = A \cosh K'y + B \sinh K'y \quad (32)$$

where

$$K' = \left\{ \frac{G}{Eth} \right\}^{1/2} \quad (33)$$

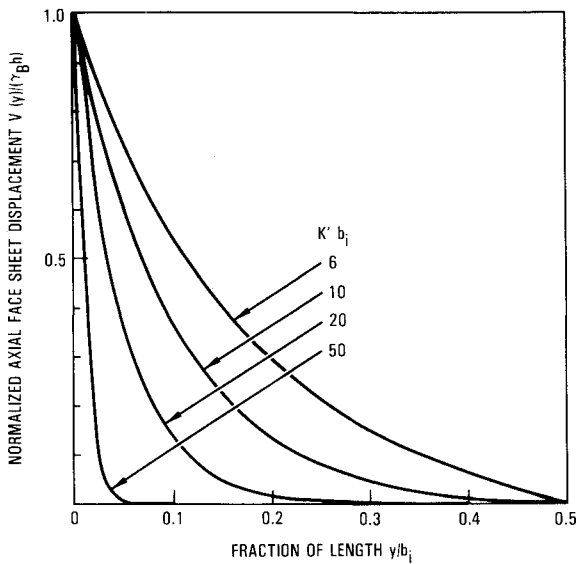


Fig. 9 Variation of the face sheet axial displacement along the honeycomb beam with honeycomb core shear stiffness.

With the edge conditions

$$\begin{aligned} v &= 0 \text{ at } y = b_i/2 \\ v &= +\gamma_B h \text{ at } y = 0 \end{aligned} \quad (34)$$

the axial displacement becomes

$$v(y) = \gamma_B h \cosh K'y - \frac{\cosh(K'b_i/2)}{\sinh(K'b_i/2)} \sinh K'y \quad (35)$$

where the shear angle γ_B is given by

$$\begin{aligned} \gamma_B &= \psi_A \left\{ \cos^2 \chi + \frac{E_p t_p b_i \cos^2 \chi \sin \chi}{2E_i t h} \right. \\ &\quad \left. + \frac{K'b_i}{2} \left[\frac{\cosh(K'b_i/2) - 1}{\sinh(K'b_i/2)} \right] \right\} \quad (36) \end{aligned}$$

The variation of the normalized axial displacement of the inner face sheets, $v(y)/\gamma_B h$, is illustrated in Fig. 9 for various values of the shear parameter $K'b_i$. For a very stiff honeycomb core, as represented by a high value of the shear parameter in Fig. 9, the shear deformation is limited to the edges of the honeycomb core.

The variation of the membrane strain in the inner face sheet can be obtained from

$$T(y) = T_i - \frac{G}{h} \int_0^y v(y) dy \quad (37)$$

using the relationship $\epsilon(y) = T(y)/Et$. The inner face sheet membrane strain ϵ_{Mc} at the center of the beam is obtained from Eq. (37) by integrating between the limits 0 to $b_i/2$. After some manipulation, the following ratio of beam center membrane strain to corresponding membrane strain ϵ_{Mi} with rigid pans is obtained

$$\frac{\epsilon_{Mc}}{\epsilon_{Mi}} = \left\{ 1 - \left[\cos^2 \chi + \frac{K'b_i}{2} \left\{ \frac{\cosh(K'b_i/2) - 1}{\sinh(K'b_i/2)} \right\} \right] \frac{\gamma_B}{\psi_A} \right\} \quad (38)$$

The inner-to-outer-face-sheet strain in Eq. (20) now becomes

$$\left| \frac{\epsilon_{Mc} + \epsilon_{Bi}}{\epsilon_{Bo}} \right| = 1 + \frac{4\epsilon_{Mc}}{n\pi\epsilon_{Mi}} \quad (39)$$

| PANEL | THEORY | MEASURED | b_i | χ° | h | REFERENCE |
|-------|------------|----------|--------|----------------|---------|-----------|
| #1 | ● | ○ | 470 mm | 30 | 25.4 mm | 6 |
| #2 | ■ | □ | 470 mm | 30 | 25.4 mm | |
| #3, 4 | ◆ | ◇ | 515 mm | 30 | 12.7 mm | |
| #5, 6 | ▼ | ▽ | 515 mm | 45 | 15.9 mm | 5 |
| | R - RANDOM | | | S - SINUSOIDAL | | |

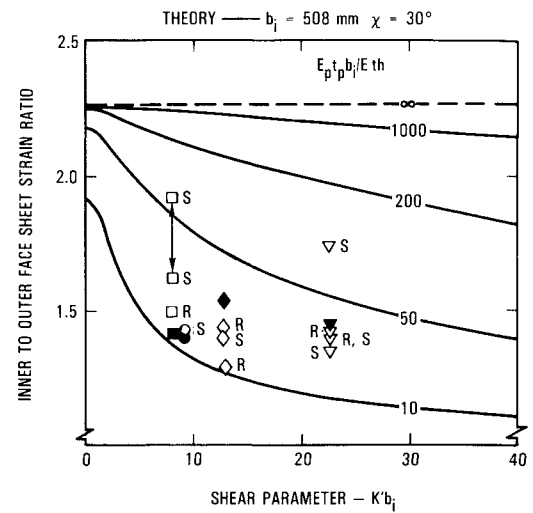


Fig. 10 Comparison of predicted and measured panel center inner-to-outer-face-sheet strain ratio with extensionally flexible closeout pans.

The experimentally measured and the theoretically predicted [Eq. (39)] inner-to-outer-face-sheet strain ratios for the aluminum honeycomb panels in Refs. 5 and 6 are illustrated in Fig. 10 as a function of the parameters $K'b$ and $E_p t_p b_i / E t h$. The extensional stiffness of the pan is represented by the parameter $E_p t_p$. The experimental data were obtained with both sinusoidal and random acoustic excitation, as described in Refs. 5 and 6.

The correlation is generally quite good. The data points showing the greatest deviation from the theoretically predicted values were obtained at low excitation levels and are therefore susceptible to signal-to-noise ratio errors. The theoretical variation of the inner-to-outer-face sheet strain ratio with the above parameters for a 30-deg beveled edge angle and a 508-mm inner face sheet length (b_i) has been superimposed on the above data in Fig. 10 to illustrate the effect of these parameters.

Effective Honeycomb Core Shear Modulus

An estimate of the contribution from the pan to the shear stiffness of the honeycomb core can be obtained from Eq. (26). The honeycomb beam with beveled edges is replaced by an equivalent honeycomb beam having no beveled edges but a core with an increased core shear modulus G' . Therefore,

$$T_p \cos \chi + \int_0^{b_i/2} q dy = \int_0^{b_i/2} q' dy \quad (40)$$

where q' represents the equivalent shear stress given by

$$q' = G' [v(y)/h] \quad (41)$$

On solving Eq. (40), the equivalent shear modulus becomes

$$G' = \frac{K'E_p t_p \cos^2 \chi \sin \chi \sinh(K'b_i/2)}{\cosh(K'b_i/2) - 1} + G \quad (42)$$

The variation of the equivalent shear modulus with the nondimensional parameter $K'b_i$ is illustrated in Fig. 11 for

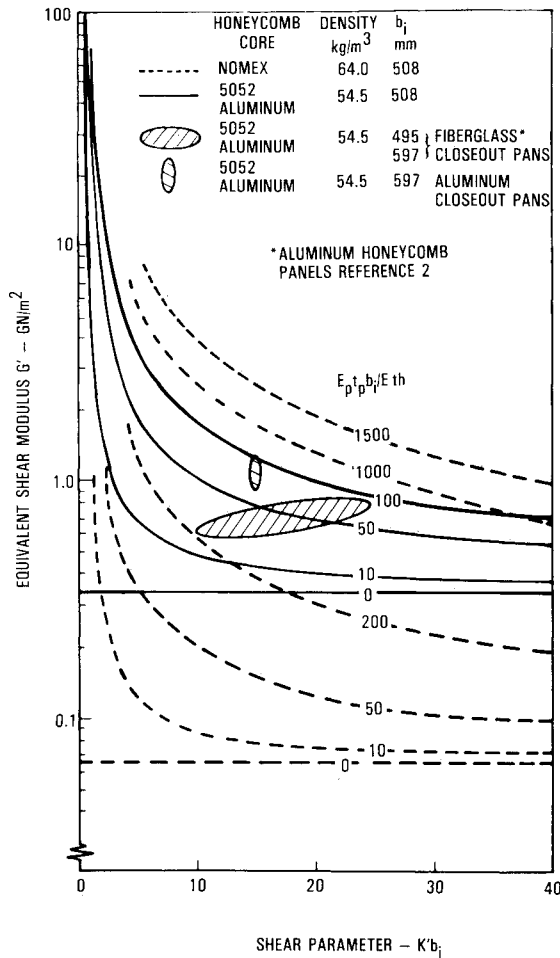


Fig. 11 Effect of honeycomb beveled edge closeout pan extensional stiffness on the honeycomb core shear modulus.

the 5052 aluminum and Nomex honeycomb cores with densities of 54.5 kg/m³ and 64 kg/m³, respectively. A typical range for the equivalent shear moduli of the aluminum honeycomb panels in Ref. 2 is included in Fig. 11. The effect of the closeout pan stiffness is seen to be quite significant, especially for the aluminum closeout pans. The increased core shear stiffness could account for the relatively good correlation, Fig. 4, obtained for the fundamental mode natural frequency with Eq. (2).

Correlation of Predicted and Measured rms Strain

The theoretically predicted inner face sheet strains in Fig. 5 have been recalculated with Eqs. (8) and (39), since Eq. (8) is applicable only to bending induced strain. The inclusion of Eq. (39) produces an overestimate of the panel center strain by a factor of 1.4. In the correlation between the measured and the recalculated strains illustrated in Fig. 12, the predicted strains have been divided by the 1.4 factor. The diagonal line now passes through the middle of the data points from Ref. 2. This suggests that an improvement in the correlation has been obtained. The 1.4 factor is probably due to the local distortion (Fig. 8) produced at the beveled edge by the unbalanced force and moment. This local distortion and its effect on the strain distribution are difficult to predict theoretically.

The equation for predicting the inner face sheet strain at the center of the honeycomb panel, after modification by the empirical constant and the linear membrane theory, can now be written as

$$\epsilon_{yci} = \frac{\bar{B}_y}{\pi^2} \frac{h+2t}{b^2 M} \left(\frac{G_f}{\delta_r} \right)^{1/2} \frac{1}{f_r^{3/2}} \frac{(1 + \cos\{2\pi f_r a/c\})^{1/2}}{[1 - (2f_r a/c)^2]} \quad (43)$$

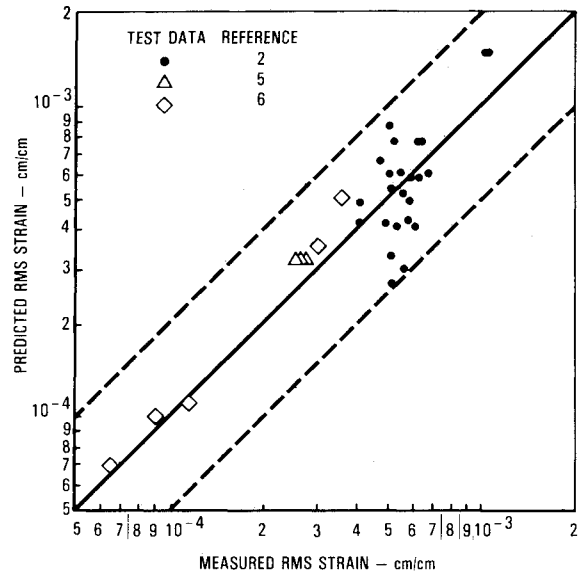


Fig. 12 Comparison of predicted and measured inner face sheet rms strains at panel center.

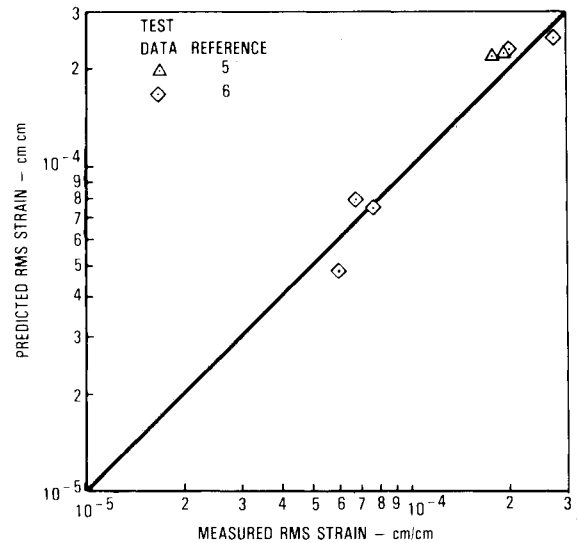


Fig. 13 Comparison of predicted and measured outer face sheet rms strains at panel center.

where

$$\bar{B}_y = \frac{1}{1.4} \left[1 + \frac{4\epsilon_{Mc}}{n\pi\epsilon_{Mi}} \left\{ \frac{1 - \frac{b}{n\pi h} \left(\frac{\delta_o}{w_n} \right)}{\left(1 + \frac{2t}{h} \right) \left(\frac{b_i}{b} \right)} \right\} \right] \quad (44)$$

and $\epsilon_{Mc}/\epsilon_{Mi}$ is given by Eq. (38). Equation (44) includes the more accurate expression for the inner-to-outer-face-sheet strain ratio and assumes that the panel is simply supported at the end of the beveled edges ($\ell=0$). It also includes the effect of frame lateral flexibility, δ_o/w_n . In the comparison in Fig. 12, rigid panel edge supports were assumed and the remaining terms in the inner brackets of Eq. (44) were taken as unity. The effect of this latter assumption on the predicted strains is very small.

As a result of the good agreement demonstrated in Fig. 12, it should also be possible to predict the corresponding outer face sheet rms strain using Eq. (43), but with \bar{B}_y replaced by

$$\bar{B}_{yo} = \frac{1}{1.4} \left\{ 1 + \frac{4b}{n^2\pi^2 h} \left(\frac{\delta_o}{w_n} \right) \right\} \quad (45)$$

The predicted and the measured outer face sheet strains are illustrated in Fig. 13. The very limited outer face sheet rms strain data^{5,6} show good correlation with theory. The limited amount of these test data is due to the fact that the outer face sheet strains are usually much lower than the inner face sheet strains and are therefore not recorded in test reports beyond the initial strain review.

Conclusions

The equivalent simply supported theory provides a simple but effective approach for analyzing the vibration response of complex aluminum honeycomb panels. The beveled edge closeout pan has been shown to provide the predominant contribution to the shear stiffness of the honeycomb core. As a result, it has been possible to predict with good accuracy the fundamental mode natural frequency of stiffened aluminum honeycomb panels, using the equivalent simply supported theory with infinite core shear stiffness.

The rotation of the beveled edges has been shown to introduce a linear membrane strain into the inner face sheet, in the symmetric modes of honeycomb panels with stiff lateral edge supports, superimposed on the bending strain. This combined strain is highest in the fundamental mode, with a theoretical maximum inner-to-outer-face-sheet strain ratio approaching 2.3. Since the predominant response to random acoustic loading is obtained in the fundamental mode, the theory explains why face sheet acoustic fatigue failures occur predominantly in the inner face sheet of rigidly mounted honeycomb panels.

The stiffness of the beveled edge closeout pan and of the honeycomb panel lateral edge supports affects the inner-to-outer-face-sheet strain ratio. The amount of shear in the honeycomb core is also determined by the extensional stiffness of the beveled edge closeout pans. With a suitable design, the contribution to the core shear stiffness from the closeout pan could be more than an order of magnitude greater than that from the honeycomb core. Increasing the closeout pan extensional stiffness also increases the inner-to-outer-face-sheet strain ratio. On some aircraft-mounted honeycomb panels, the lateral edge support stiffness could be considerably less than that achieved with test frames. The inner-to-outer-face-sheet strain ratio could, under these circumstances, approach unity by the sharing of the membrane strain between the inner and outer face sheets, in spite of using stiff closeout pans. The beveled edges are also responsible for introducing a small coupling between the bending and in-plane vibrations in honeycomb panels with laterally flexible edge supports.

Experimentally verified equations have been developed to predict the critical rms strains at the center of the honeycomb panel. The linear membrane strain and beveled edge closeout pan stiffness effects are included in these equations.

The only deviation in the theory involves the use of an empirical constant of 1.4 to reduce the predicted face sheet strain levels to averaged measured strain levels. The equations can be used to predict the critical face sheet rms strains with reasonable confidence even beyond the range of geometrical parameters included in the correlation, since theoretically correct exponents of well-established structural, excitation, and damping parameters are retained in the equations.

Acknowledgments

This paper presents part of the work conducted by the author for a Ph.D. degree with the Institute of Sound and Vibration Research, Southampton University, England. The author wishes to express his gratitude to the Lockheed-California Company and to Professors B. L. Clarkson and R. G. White for providing the opportunity to perform this work.

References

- ¹Rieben, T. R., "Sonic Fatigue Testing and Development of Aircraft Panels," WADC-TR-57-513, Nov. 1957, p. 283.
- ²Ballentine, J. R., Rudder, F. F., Mathis, J. T., and Plumblee, H. E., "Refinement of Sonic Fatigue Structural Design Criteria," AFFDL-TR-67-156.
- ³Sweers, J. E., "Prediction of Response and Fatigue Life of Honeycomb Sandwich Subjected to Acoustic Excitation," *Acoustic Fatigue in Aerospace Structures*, Syracuse University Press, NY, 1965, p. 389.
- ⁴Soovere, J., "Theory for Predicting Dynamic Edge Strain in Stiffened Honeycomb Panels," *Proceedings of Tenth Biennial ASME Design Engineering Division Conference on Mechanical Vibration and Noise*, ASME, Vol. H-331, 1985.
- ⁵Rasor, J. E., "Sonic Fatigue Test of 0.045 Lb/Ft² Adhesive for Honeycomb Sandwich Panels," Lockheed-Georgia Company, Marietta, GA, Lockheed Rept. ER-9028, March 1967.
- ⁶Rasor, J. E., "Sonic Fatigue Tests on Low Density Core Honeycomb Panels," Lockheed-Georgia Company, Marietta, GA, Lockheed Rept. ER-8601, July 1966.
- ⁷Richards, E. J. and Mead, D. J., *Noise and Acoustic Fatigue in Aeronautics*, John Wiley & Sons, New York, 1968.
- ⁸Bolotin, V. V., "Dynamic Edge Effect in the Oscillation of Plates," *Inzhernyyi Sbornik*, Vol. 31, 1960, pp. 3-14.
- ⁹Arnold, R. N. and Warburton, G. B., "The Flexural Vibration of Thin Cylinders," *Proceedings of the Institute of Mechanical Engineering*, Vol. 167, 1973, p. 62.
- ¹⁰Szechenyi, E., "The Response of and the Acoustic Radiation for Panels Excited by Turbulent Boundary Layers," AFFDL-TR-70-94, June 1970.
- ¹¹Powell, A., "On the Fatigue Failure of Structures Due to Vibrations Excited by Random Pressure Fields," *Journal of the Acoustical Society of America*, Vol. 30, Dec. 1958, pp. 1130-1135.
- ¹²Powell, A., "On the Response of Structures to Random Pressure and to Jet Noise in Particular," *Random Vibration*, M.I.T. Press, Cambridge, MA, and John Wiley & Sons, New York, 1959.